FE-1787-11
Distribution Category UC-90e

MODELING OF A FLUIDIZED BED COMBUSTOR WITH IMMERSED TUBES

Quarterly Report for the
Period March-August, 1978

S.C. Saxena

and

N.S. Grewal

University of Illinois at Chicago Circle
Department of Energy Engineering
P.O. Box 4348, Chicago, IL 60680

Date Published-December 1978

PREPARED FOR THE UNITED STATES
ENERGY RESEARCH AND DEVELOPMENT ADMINISTRATION

Under Contract No. EX-77-C-01-1787

OBJECTIVE AND SCOPE OF WORK

A mathematical model of a fluidized-bed combustor will be developed which will include coal combustion phenomena and will incorporate basic mass transport relationships, bubble mechanics, heat transfer and configuration effects. A cold model test bed will be designed, constructed and operated to generate data in support of the effort in developing the mathematical model. In particular, experiments will provide data concerning heat transfer effects of tubes and tube bundles in fluidized beds, bubble formation, dispersion etc.

SUMMARY OF PROGRESS TO DATE

The total heat transfer coefficient is measured between electrically heated bundels of tubes (12.7 and 28.6 mm diameter) and a square fluidized bed (0.305 x 0.305m) of silica sand ($\bar{d}_p$ = 167 and 504 μm) and alumina (259 μm). The staggered tube bundle has its tubes located at the vertices of equilateral triangles. The effect of particle size, mass fluidizing velocity (up to 0.66 kg/m^2s), tube pitch (1.75 to 9.00 times the tube diameter, and bed height on heat transfer rate is investigated.

DETAILED DESCRIPTION OF TECHNICAL PROGRESS

Experiments are carried out in a square fluidized bed (0.305 x 0.305 m) which has been described in previous reports [1,2]. The horizontal tubes in a bundle are arranged in an staggered array. The height of the bottom row of tubes in a bundle is kept at 132 mm above the distributor plate in all experiments. The relative tube pitch, P/D_T, is varied from 1.75 to 9 as shown in Table 1.

Silica sand and alumina are used as bed material. The average diameter, $\bar{d}_p$, of the particles is obtained by sieve analysis and the following relation:

$$d_p = \frac{1}{\sum_i (w/d_p)_i} \qquad (1)$$

The density of solid particles, ρ_s, is determined by the displacement of methanol in a graduated cylinder. The particle density and diameter are given in Table 2. The minimum fluidizing velocity for a given bed of solids is determined in the conventional method (3,4) by measuring the bed pressure drop as a function of fluidizing velocity. Minimum mass fluidizing velocity, G_{mf}, for silica sand ($\bar{d}_p$ = 167 and 504 μm) and alumina (d_p = 259 μm) are also listed in Table 2. The cumulative size distribution of silica sand and alumina is shown in Table 3.

The heat transfer tube designs are shown in Figs. 1 and 2. The tube is heated by an electric calrod heater. Three iron-constantan thermocouples are bonded to the tube surface in milled grooves with technical quality copper cement at locations shown in the figures. The ends of the tubes are provided with nylon supports to reduce axial heat loss. The end heat loss is estimated to be less than one per cent. Four thermocouples are used to measure the bed temperatures. The design of the side plates used to mount the horizontal tubes is shown in Figs. 3 and 4. With single tubes the height of the tube center is kept 213 mm above the distributor plate. In all runs for bundle of tubes, only the middle tube of each row is heated. The bed temperature and pressure probes are also mounted on these side plates and their locations are also shown in Figs. 3 and 4.

The settled bed height in all experiments is 35 cm. The steady state is assumed to be established when the bed temperature variation is less than 0.5K per hour. The temperatures at each of the locations are recorded over a period of time and an average value is used.

The total heat transfer coefficient, h_w, is determined from the following relation:

$$h_w = \frac{Q}{A_w(T_w-T_b)} \tag{2}$$

The pressure loss in a fluidized bed, ΔP, is equal to the weight of the bed per unit cross-sectional area i.e.

$$\Delta P = H(1-\varepsilon)\ (\rho_s-\rho_f) \tag{3}$$

Since ΔP, H, ρ_s,ρ_f are know, the values of ε are calculated from the above relation.

The maximum error in the measurement of heat transfer coefficient is estimated to be ±6%. The repeatability of heat transfer measurement is found to be ± 2 per cent.

The heat transfer coefficients for smooth tubes are shown plotted as a function of superficial mass fluidizing velocity in Figs. 5 through 10. It is seen that the heat transfer coefficient increases with increase in the value of G. The increase is rapid in the beginning and slows down as the superficial velocity is further and further increased. The heat transfer coefficient attains its maximum value at some higher fluidizing velocity. The initial increase is due to decrease in particle residence time at the tube surface due to particle mixing caused by rising bubbles in the fluidized bed. Further, the residence time of particles decreases with increase in the value of G due to increase in bubble induced particle circulation. However, at larger values of G, the rate of increase in h_w decreases due to increase in surface area of the tube being engulfed by rising bubbles.

It is seen from Fig. 5 that for 167 μm silica sand a single curve can be used to represent the heat transfer coefficient for a 12.7 mm single tube and bundle of tubes with relative tube pitch 4.5 to 9 with a maximum deviation from the average curve of about 2% which is also the reproducibility of our measurement of heat transfer coefficient. The value of $h_{w\ max}$ for a bundle of tubes when relative pitch is 2.25 is about 5% smaller as compared to the value of $h_{w\ max}$ for a single tube.

It may be noted from Fig. 6 that there is no effect of P/D_T on h_w for tube bundles for silica sand ($\bar{d}_p$ = 504 μm) as long as P/D_T is varied from 9 to 4.5. A further decrease in the relative tube pitch to 2.25 results in the decrease in the value of $h_{w\ max}$ by about 7% as compared to a single tube.

The effect of relative tube pitch on h_w for alumina ($\bar{d}_p$ = 259 μm) is shown in Fig. 7. A single curve can be used to represent the data for a single tube and tube bundle with relative pitch of 4.5. However, when the relative pitch is reduced to 2.25, the value of $h_{w\ max}$ for the tube bundle is about 6% smaller as compared to the single tube.

It is to be noted that the values of h_w are larger for smaller particles in accordance with the findings of the previous investigators (5). The values of $h_{w\ max}$ for a single tube and silica sand and alumina are compared with the following correlation given by Zabrodsky (5).

$$h_{w\ max} = 35.7\ k_f^{0.6}\ \rho_s^{0.2}\ \bar{d}_p^{\ -0.36} \tag{4}$$

The derivation of experimental values of $h_{w\ max}$ from the calculated values from Eq. 4 are shown in Table 4. The agreement is considered reasonable in the light that the above correlation has an uncertainty of ± 18%.

The dependence of h_w for a bundle of tubes (D_T = 0.02858 mm) for silica sand ($\bar{d}_p$ = 167 and 504 μm) and alumina ($\bar{d}_p$ = 259 μm) is shown in Figs. 8

through 10. In all the three figures, a single curve can be seen to represent the data for the single tube and the tube bundle with relative pitch equal to 3.50. The decrease in $h_{w\ max}$ for bundle of tubes with relative pitch of 1.75 as compared to a single tube is about 6, 8, and 8 per cent for silica sand ($\bar{d}_p$ = 167 and 504 μm) and alumina ($\bar{d}_p$ = 259 μm) respectively.

The values of h_w for a bundle of tubes with $P/\bar{d}_p$ = 1.75 for alumina ($\bar{d}_p$ = 259 μm) as a function of G is shown plotted in Fig. 11 for two bed heights of 25 and 36 cm. A single curve can be used to represent data for both bed height with maximum deviation of ± 1 per cent.

CONCLUSION

The experimental work on development will provide a thorough base for resolving the mechanism of heat transfer in relation to an immersed array of horizontal tubes. This information will help in the optimal design of fluidized-beds and their scale-up.

NOMENCLATURE

A_w	surface area of a smooth tube, m^2
$\bar{d}_p$	average particle diameter defined by Eq. (1)
d_{pi}	average diameter of the succesive screens, m
D_T	outside diameter of smooth tube or fin tip diameter of a finned tube, m
G	mass fluidizing velocity, kg/m^2s
G_{mf}	velocity at minimum fluidizing conditions, kg/m^2s
h_w	total heat transfer coefficient for smooth tube, W/m^2K
$h_{w\ max}$	maximum heat transfer coefficient for smooth tube, W/m^2K
H	distance between pressure probes, m
k_f	thermal conductivity of the fluidizing air, W/m K
P	center-to-center distance (pitch) between adjacent tubes in a bundle, m
Q	total heat flow from tube to bed, W
T_b	average bed temperature, K
T_w	average surface temperature of the heat transfer tube, K
w_i	weight of particles between two successive screens, g

Greek Symbols

ΔP	pressure drop across the bed, kPa
ε	bed porosity, m
ρ_f	fluidizing air density, kg/m^3
ρ_s	particle density, kg/m^3

REFERENCE

1. S.C. Saxena, A. Rehmat and N.S. Grewal, Modeling of a Fluidized Bed Combustor with Immersed Tubes, University of Illinois at Chicago Circle Quarterly Report for the period June-August 1975 submitted to United States Energy Research and Development Administration under contract No. E(49-18)-1787.

2. S.C. Saxena, A. Rehmat, N.S. Grewal and T.P. Chen, Modeling of a Fluidized Bed Combustor with Immersed Tubes, University of Illinois at Chicago Circle Quarterly Report for the period September-November 1975 submitted to United States Energy Research and Development Administration under contract No. E(49-18)-1787.

3. D. Kunii and O. Levenspiel, "Fluidization Engineering," John Wiley & Sons, New York, 1969.

4. N.S. Grewal and S.C. Saxena, "Investigations of Heat Transfer From Immersed Tubes in a Fluidized Bed," Proc. Fourth National Heat and Mass Transfer Conference, Paper No. HMT-7, pp. 53-57, India (1977).

5. S.S. Zabrodsky, "Hydrodynamics and Heat Transfer in Fluidized Beds," The M.I.T. Press, Cambridge, Massachusetts, 1961.

TABLE 1

Material	$\bar{d}_p$ μm	ρ_s kg/m^2	Relative Pitch, P/D_T	Number of Rows in a Vertical Line	Number of Tubes in a Bundle	D_T,mm
Silica Sand	167	2675	2.25	3	23	12.7
			4.50	3	11	12.7
			6.75	3	8	12.7
			9.00	3	5	12.7
			2.25	5	38	12.7
			4.50	5	18	12.7
Silica Sand	504	2670	2.25	3	23	12.7
			4.50	3	11	12.7
			6.75	3	8	12.7
			9.00	3	5	12.7
			2.25	5	38	12.7
			4.50	5	18	12.7
Alumina	259	4015	2.25	3	23	12.7
			4.50	3	11	12.7
			1.75	3	14	28.6
			3.50	3	8	28.6
Silica Sand	167	2675	1.75	3	14	28.6
			1.75	5	23	28.6
			3.50	3	14	28.6
Silica Sand	504	2670	1.75	3	14	28.6
			1.75	5	23	28.6
			3.50	3	8	28.6

TABLE 2

Particle Diameter, Density and Minimum Fluidizing Velocities at 294 K

Material	$\bar{d}_p$ μm	ρ_s kg/m^3	U_{mf} cm/s	G_{mf} kg/m^{2}s
Silica Sand	167	2675	2.7	0.0325
Silica Sand	504	2670	22.0	0.0264
Alumina	259	4015	10.4	0.125

TABLE 3

Cumulative Particle Size Distribution

Sieve Dia (μm)	Percent Less Than Stated Size		
	Silica Sand		Alumina
	$\bar{d}_p$ = 167 μm	$\bar{d}_p$ = 504 μm	$\bar{d}_p$ = 259 μm
850	—	100.0	—
600	—	89.8	—
500	—	47.7	—
425	—	10.9	—
355	—	0.5	100.0
300	100.0	0.2	90.5
250	94.4	—	31.6
212	85.0	—	5.7
180	62.6	—	0.7
150	26.3	—	0.3
125	6.9	—	—
105	2.6	—	—

TABLE 4

Material	d_p, μm	D_T,mm	$h_{w\,max}$ W/m^2K Experimental	Calculated From Eq. 4	% Deviation
Silica Sand	0.167	12.7	508	457	+11.1
Silica Sand	0.504	12.7	320	311	+2.9
Alumina	0.259	12.7	440	424	+3.8
Silica Sand	0.167	28.6	400	456	-8.8
Silica Sand	0.504	28.6	263	310	-8.5
Alumina	0.259	28.6	372	423	-8.8

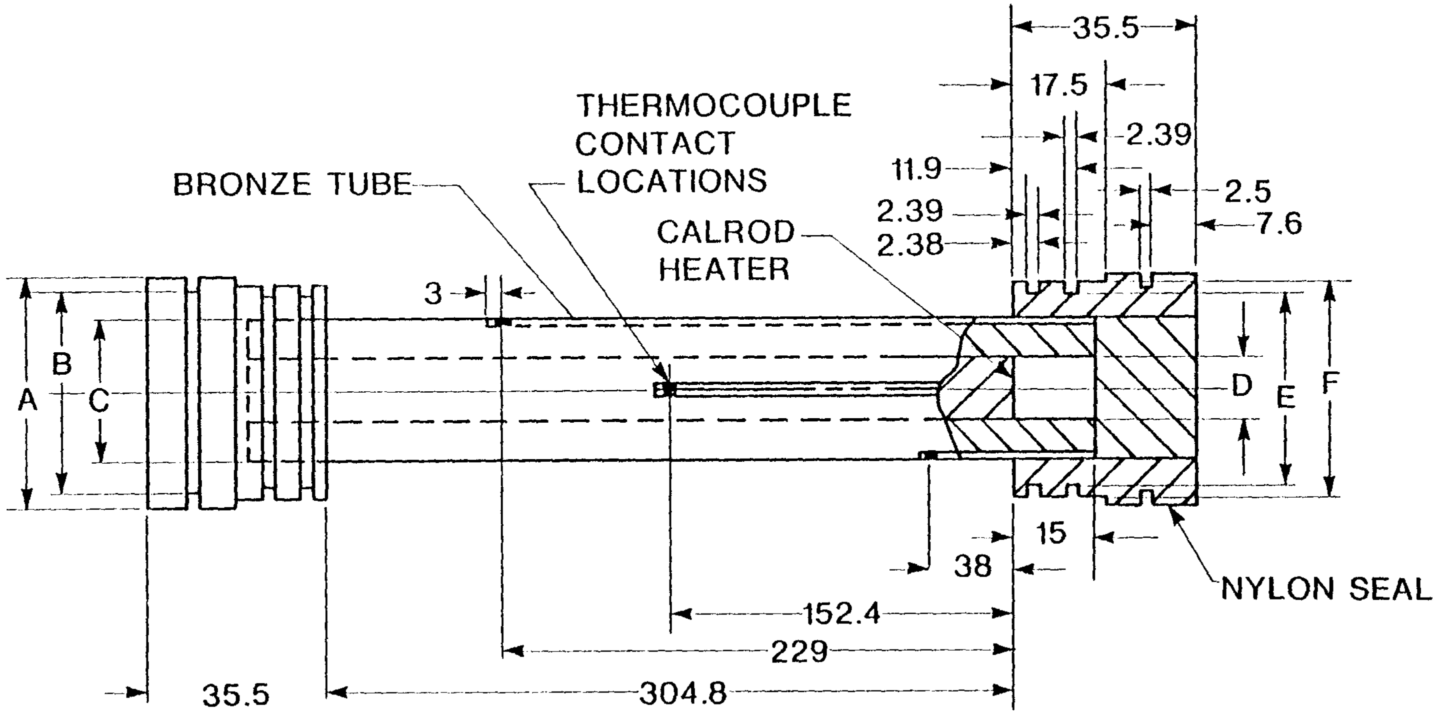

Fig. 1: Details of the heat transfer tube assembly. All dimensions are in mm. A = 25mm, B = 21mm, C = 12.7mm, D = 9.4mm, E = 19mm, and F = 22.2mm.

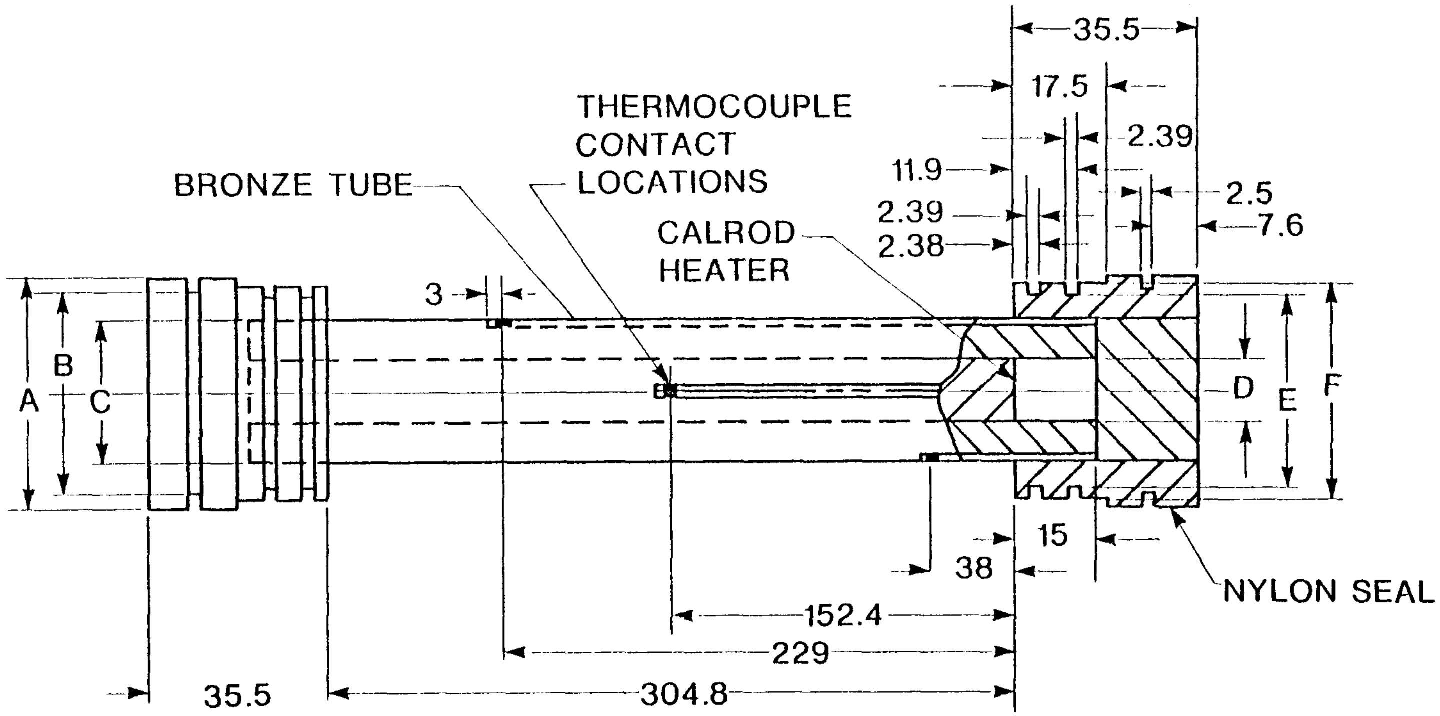

Fig. 2: Details of heat transfer tube assembly: A = 44.5, B = 40.6, C = 28.6, D = 12.7, E = 38.1, and F = 40.7. All dimensions are in mm.

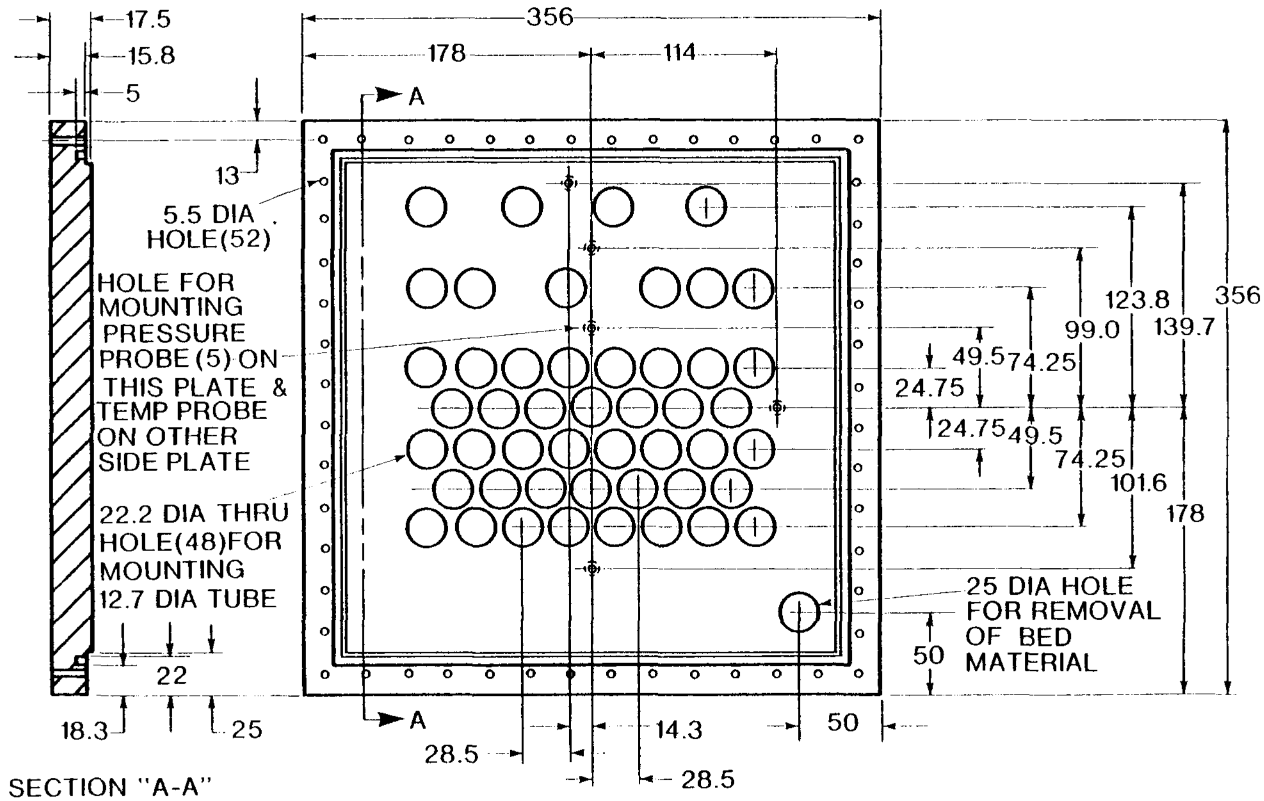

Fig. 3: Details of the plexiglas side plate for mounting the heat transfer tube bundles. All dimensions are in mm.

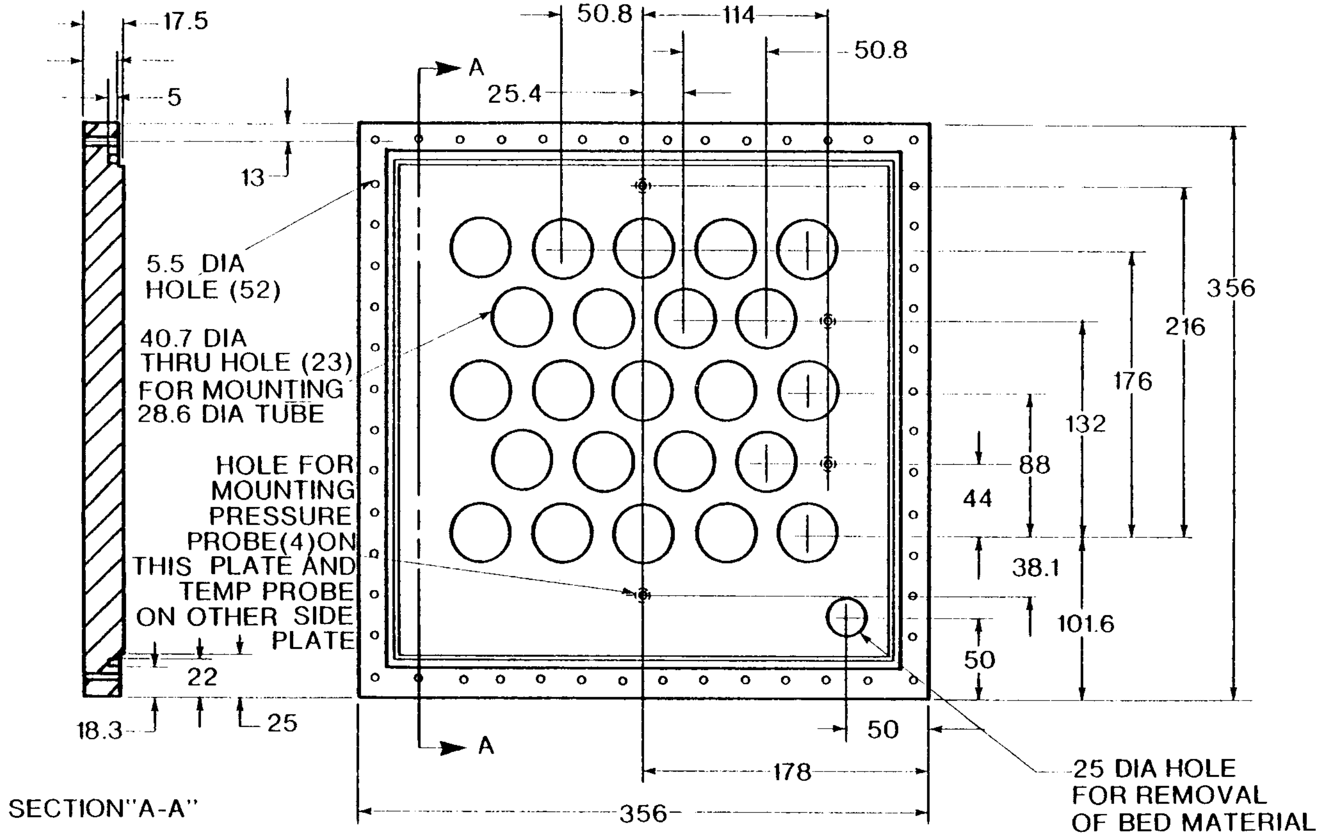

Fig. 4: Details of the plexiglas side plate for mounting the heat transfer tube bundle. All dimensions are in mm.

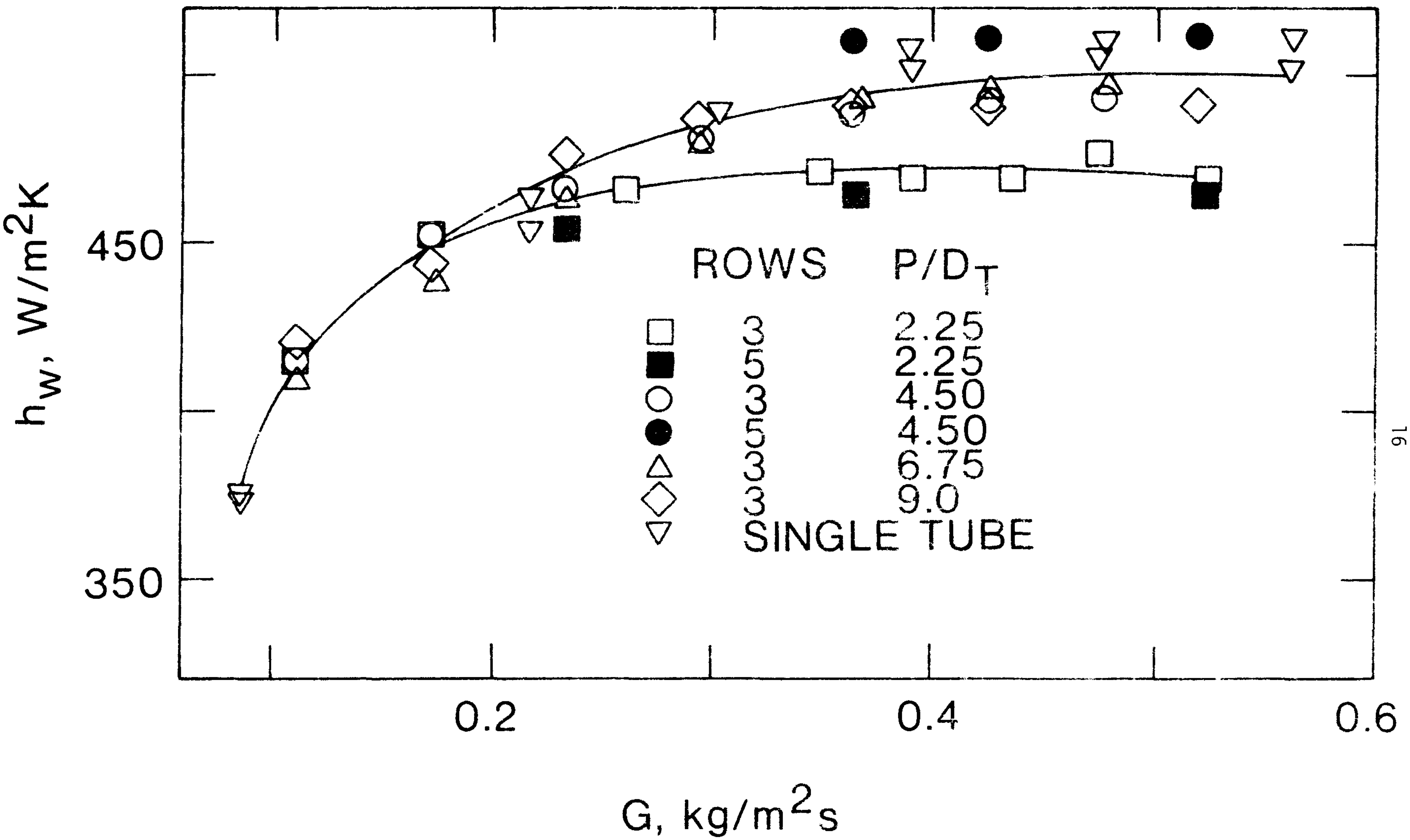

Fig. 5: Performance of 12.7 mm tubes bundle in a fluidized bed of silica sand, $\bar{d}_p$ = 167 μm.

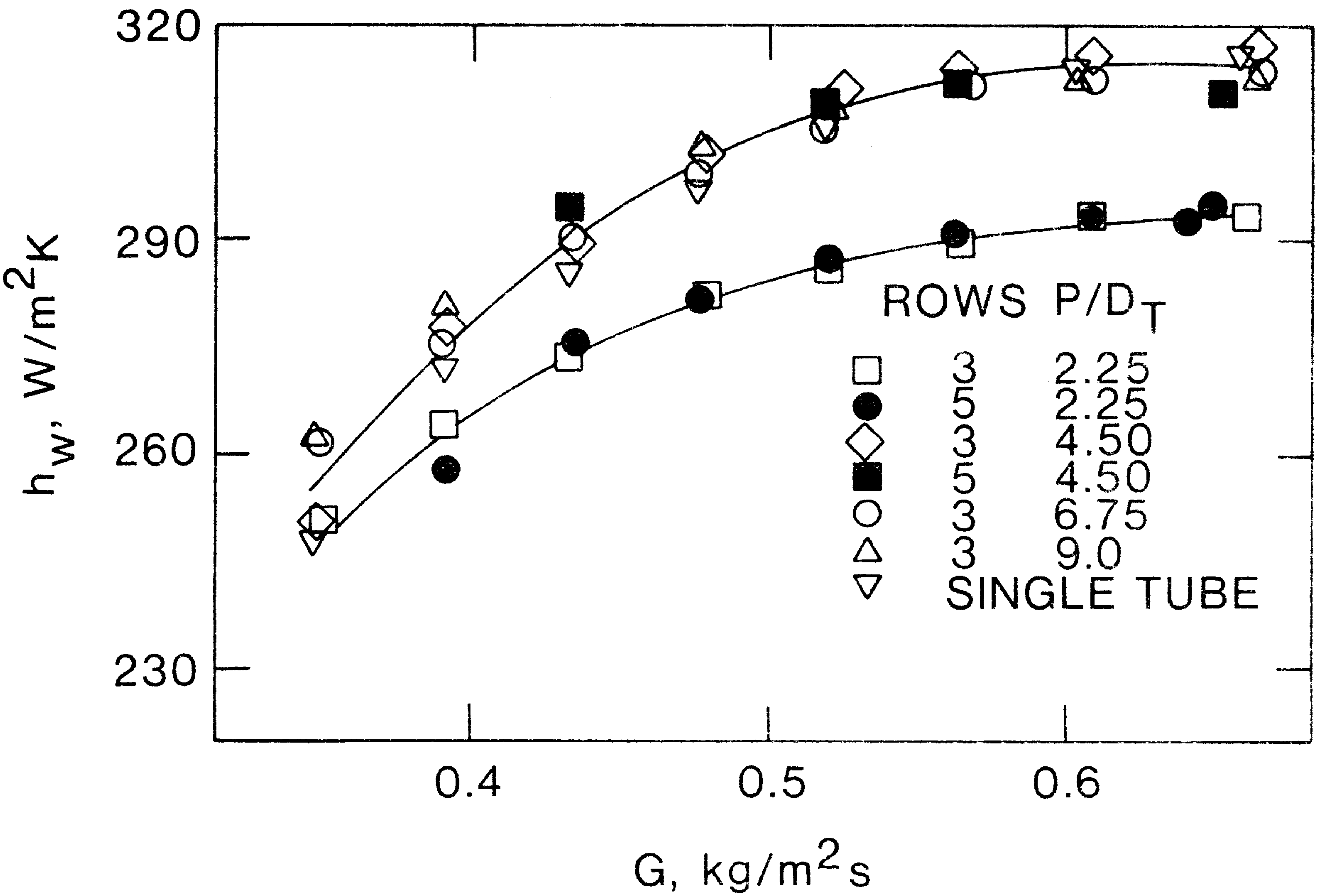

Fig. 6: Performance of 12.7 mm tubes bundle in a fluidized bed of silica sand, $\bar{d}_p$ = 504 μm.

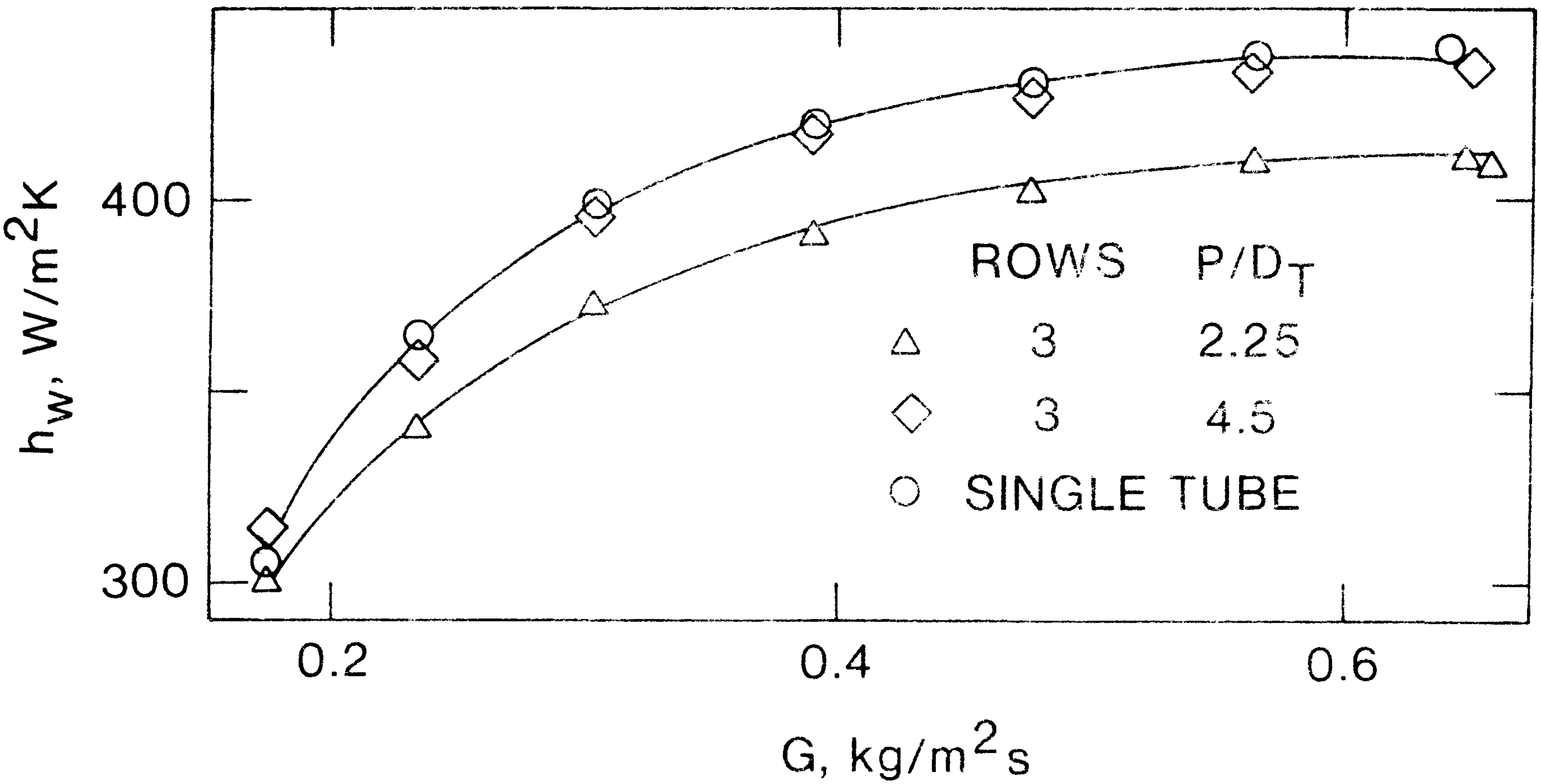

Fig. 7: Performance of 12.7 mm tubes bundle in a fluidized bed of alumina, $\bar{d}_p$ = 259 μm.

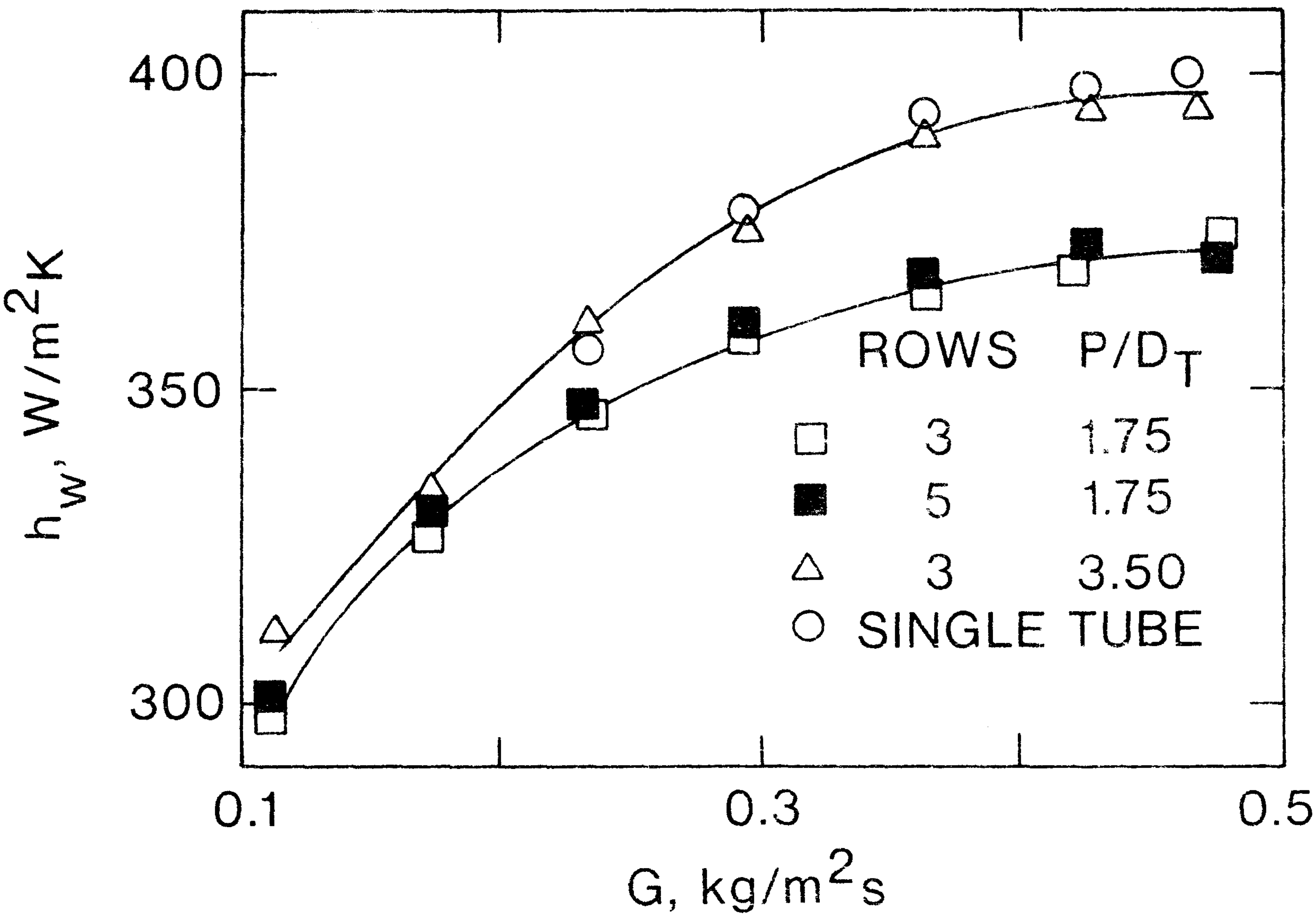

Fig. 8: Performance of 28.6 mm tubes bundle in a fluidized bed of silica sand, $\bar{d}_p$ = 167 μm.

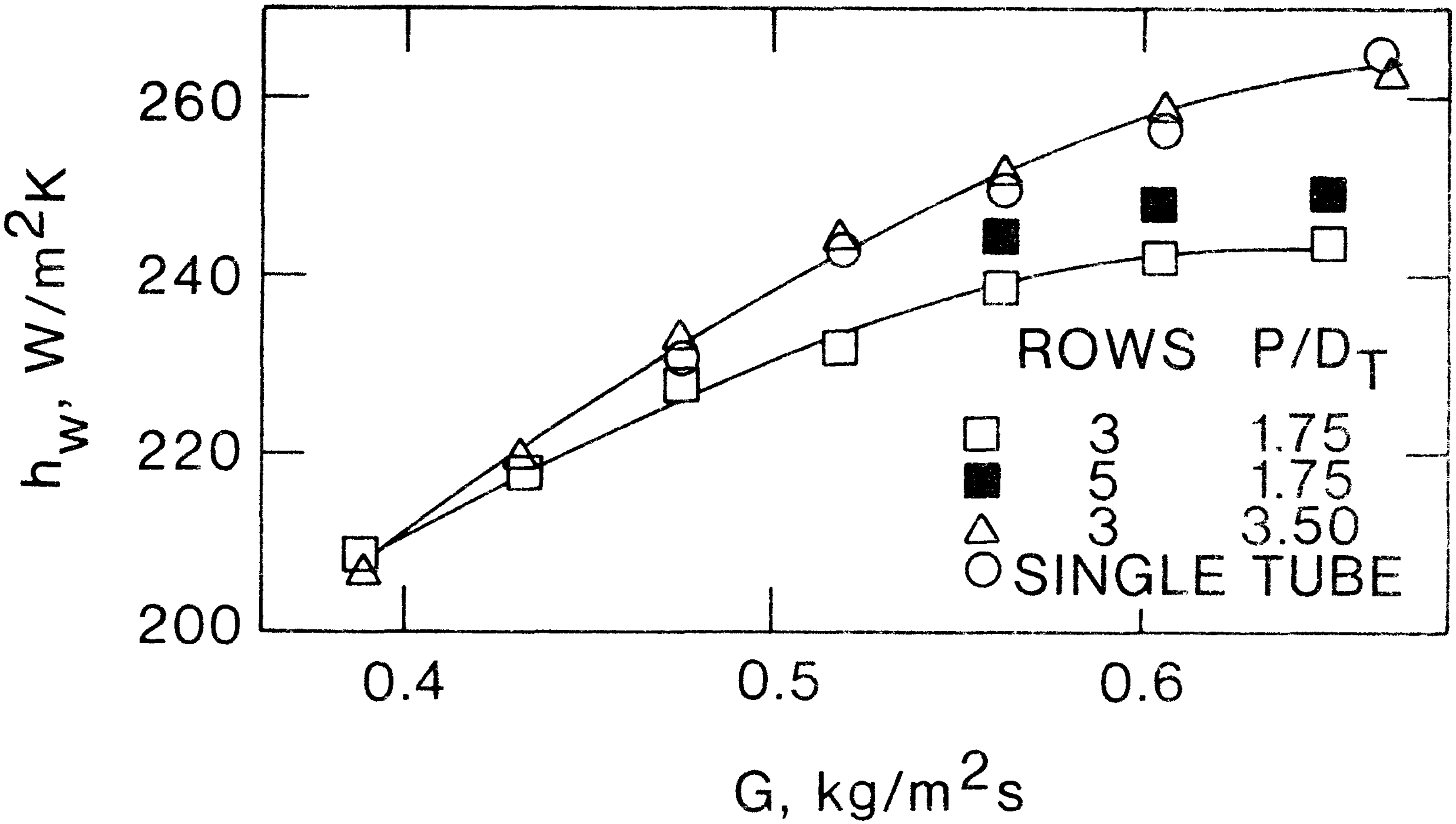

Fig. 9: Performance of 28.6 mm tubes bundle in a fluidized bed of silica sand, $\bar{d}_p$ = 504 μm.

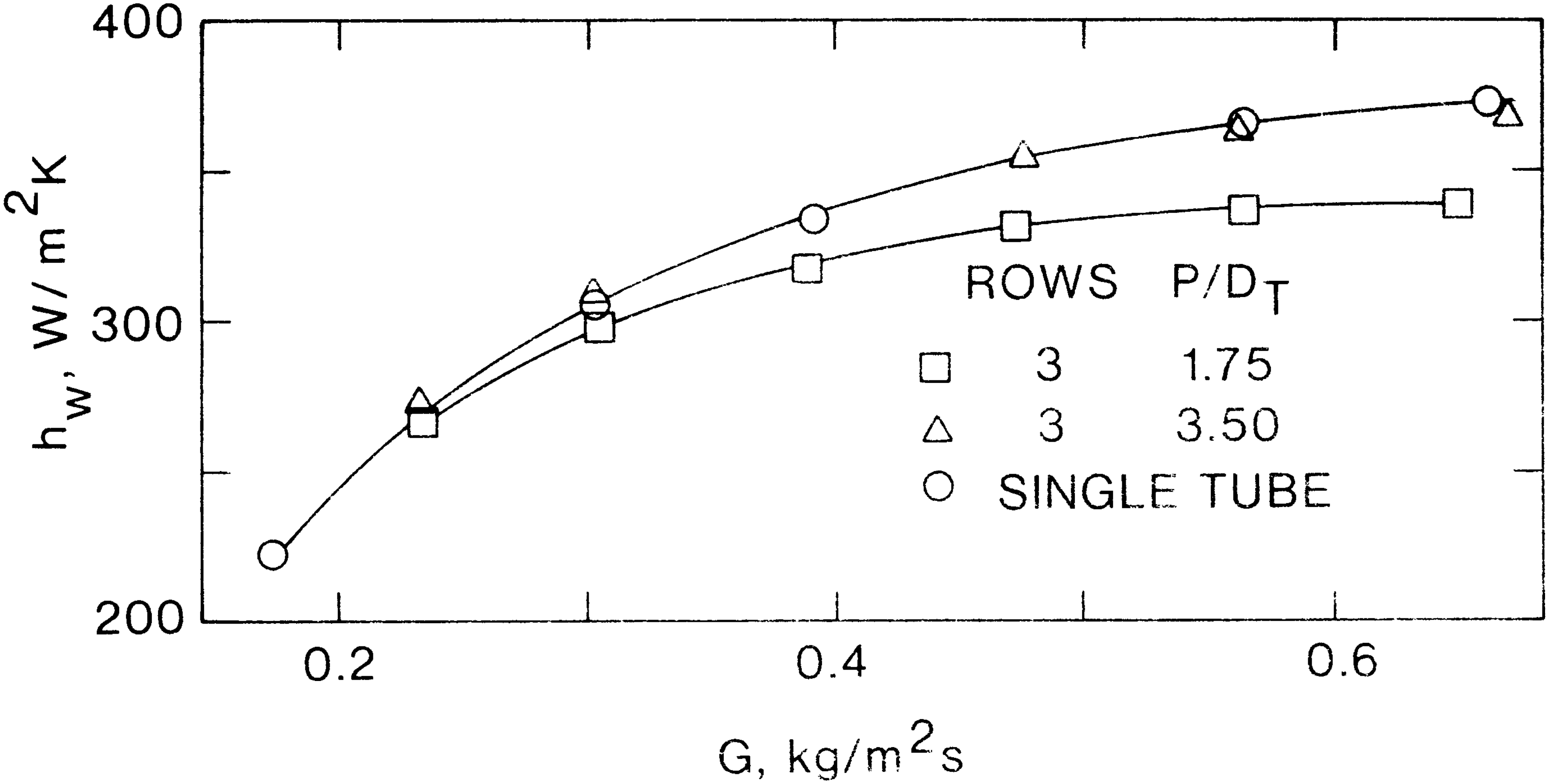

Fig. 10: Performance of 28.6 mm tubes bundle in a fluidized bed of alumina, $\bar{d}_p$ = 259 μm.

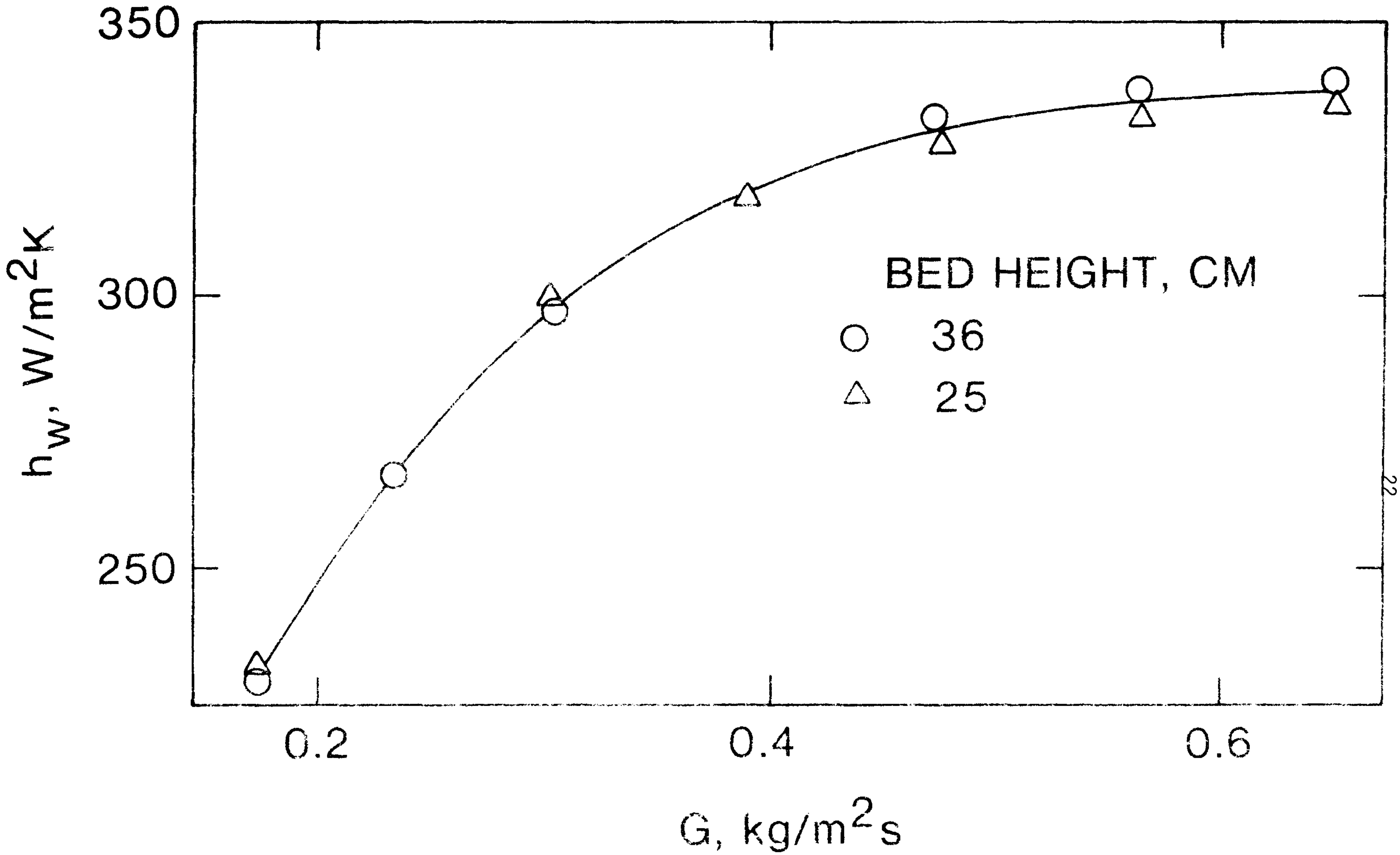

Fig. 11: The effect of bed height on h_w for a bundle of tubes (28.6 mm) of 3 rows and a bed of alumina, $\bar{d}_p$ = 259 μm.

☆U.S. GOVERNMENT PRINTING OFFICE: 1979-640-092/713